

Title	Study of interface and oxide defects in high-k/In 0.53 Ga 0.47 As n-MOSFETs
Authors	Djara, Vladimir;Cherkaoui, Karim;Schmidt, Michael;Gomeniuk, Y. Y.;O'Connor, Éamon;Povey, Ian M.;O'Connell, Dan;Monaghan, Scott;Pemble, Martyn E.;Hurley, Paul K.
Publication date	2012-05-07
Original Citation	Djara, V., Cherkaoui, K., Schmidt, M., Gomeniuk, Y. Y., O'Connor, É., Povey, I. M., O'Connell, D., Monaghan, S., Pemble, M. E. and Hurley, P. K. (2012) 'Study of interface and oxide defects in high-k/In 0.53 Ga 0.47 As n-MOSFETs', 2012 13th International Conference on Ultimate Integration on Silicon (ULIS), Grenoble, France, 6-7 March, pp. 29-32. doi: 10.1109/ULIS.2012.6193349
Type of publication	Conference item
Link to publisher's version	<a href="https://doi.org/10.1109/ULIS.2012.6193349">10.1109/ULIS.2012.6193349</a>
Rights	© 2012, IEEE. Personal use of this material is permitted. Permission from IEEE must be obtained for all other uses, in any current or future media, including reprinting/republishing this material for advertising or promotional purposes, creating new collective works, for resale or redistribution to servers or lists, or reuse of any copyrighted component of this work in other works.
Download date	2024-05-05 20:43:42
Item downloaded from	<a href="https://hdl.handle.net/10468/13404">https://hdl.handle.net/10468/13404</a>

# Study of Interface and Oxide Defects in High- $k$ /In<sub>0.53</sub>Ga<sub>0.47</sub>As $n$ -MOSFETs

V. Djara<sup>a</sup>, Student Member, IEEE, K. Cherkaoui<sup>a</sup>, M. Schmidt<sup>a</sup>, Y. Y. Gomeniuk<sup>b</sup>, É. O'Connor<sup>a</sup>, I. M. Povey<sup>a</sup>, D. O'Connell<sup>a</sup>, S. Monaghan<sup>a</sup>, Member, IEEE, M. E. Pemble<sup>a</sup> and P. K. Hurley<sup>a</sup>

(a) Tyndall National Institute, University College Cork, Cork, Ireland  
 (b) Lashkaryov Institute of Semiconductor Physics, National Academy of Sciences of Ukraine, Kiev, Ukraine  
[vladimir.djara@tyndall.ie](mailto:vladimir.djara@tyndall.ie)

**Abstract**— Interface and oxide defects in surface-channel In<sub>0.53</sub>Ga<sub>0.47</sub>As  $n$ -MOSFETs, featuring a threshold voltage,  $V_T$ , of 0.43 V, a subthreshold swing,  $SS$ , of 150 mV/dec., an  $I_{ON}/I_{OFF}$  of  $\sim 10^4$  and a source/drain resistance,  $R_{SD}$ , of 103  $\Omega$ , have been investigated using “split C-V” measurements and self-consistent Poisson-Schrödinger quasi-static C-V simulations. An integrated density of traps across the In<sub>0.53</sub>Ga<sub>0.47</sub>As band gap at the Al<sub>2</sub>O<sub>3</sub>/In<sub>0.53</sub>Ga<sub>0.47</sub>As interface,  $N_{Trap}$ , of  $\sim 7.8 \times 10^{12} / \text{cm}^2$ , has been obtained from a comparison of the theoretical and experimental quasi-static C-V responses, where  $N_{Trap}$  reflects the combined contribution of interface traps and border traps. An equivalent surface density of fixed positive oxide charges,  $N^+$ , of  $1.4 \times 10^{12} / \text{cm}^2$  is also reported. Finally, the application of the Maserjian Y-function to the Al<sub>2</sub>O<sub>3</sub>/In<sub>0.53</sub>Ga<sub>0.47</sub>As MOS system is briefly discussed.

**Keywords**— InGaAs; MOSFET; High- $k$ ; Split C-V; interface traps; oxide charges; border traps

## I. INTRODUCTION

In recent years, In<sub>x</sub>Ga<sub>1-x</sub>As  $n$ -FETs have been the focus of intense research as silicon technology is gradually reaching the limits of dimensional scaling [1]–[4]. In<sub>x</sub>Ga<sub>1-x</sub>As offers superior electron mobility but the integration of high- $k$  gate oxides still remains a major obstacle to the development of In<sub>x</sub>Ga<sub>1-x</sub>As  $n$ -FETs. In this work, we report on the analysis of interface and oxide defects using surface-channel In<sub>0.53</sub>Ga<sub>0.47</sub>As  $n$ -MOSFETs with Al<sub>2</sub>O<sub>3</sub> as a gate dielectric.

The analysis of interface traps in high- $k$ /III-V systems is typically based on capacitance and conductance measurements on MOS structures using both  $n$  and  $p$  doped semiconductor layers to allow the probing of the upper and lower band gap regions, respectively. The full band gap distribution is subsequently obtained from the combined analysis [5], [6]. The availability of full In<sub>0.53</sub>Ga<sub>0.47</sub>As surface channel MOSFETs opens new possibilities as the full quasi static C-V (QS C-V) response can, in principle, be reconstructed based on the concatenation of the gate-to-channel capacitance,  $C_{gc}$ , and gate-to-body capacitance,  $C_{gb}$ , measurements. In this work, we explore this approach, where the quasi-static limit is approximated by high frequency (2 MHz) and

low temperature (-50°C) measurements of capacitance to minimize the ac response of the interface traps. We compared the obtained  $C_g-V_g$  characteristics to the “defect free” theoretical QS C-V response obtained with a self-consistent Poisson-Schrödinger simulator [5], in order to extract the integrated density of traps across the In<sub>0.53</sub>Ga<sub>0.47</sub>As band gap at the Al<sub>2</sub>O<sub>3</sub>/In<sub>0.53</sub>Ga<sub>0.47</sub>As interface,  $N_{Trap}$ . As near interface traps (referred to subsequently as border traps) also change occupancy with the slowly varying dc bias on the gate, the approach yields the combined contribution from the interface traps density and border traps density integrated between the In<sub>0.53</sub>Ga<sub>0.47</sub>As valence and conduction band edges. Based on the analysis of the experimental and theoretical QS C-V responses, the equivalent surface density of fixed positive charges,  $N^+$ , present in the Al<sub>2</sub>O<sub>3</sub> was also extracted.

## II. MOSFET / MOSCAP FABRICATION

Surface-channel MOSFETs (Fig. 1) and MOSCAPs were fabricated on a 2-inch wafer supplied by IQE. The wafer structure was a 2-μm-thick Zn-doped ( $4 \times 10^{17} / \text{cm}^3$ )  $p$ -In<sub>0.53</sub>Ga<sub>0.47</sub>As layer grown on a  $p^+$  InP substrate. The In<sub>0.53</sub>Ga<sub>0.47</sub>As surface passivation prior to gate oxide deposition was an immersion in 10% (NH<sub>4</sub>)<sub>2</sub>S at room temperature for 20 min, which was found to be an optimum in terms of interface trap reduction and for the suppression of native oxide formation [7], [8]. The transfer time to the atomic layer deposition (ALD) reactor after surface passivation was less than 5 min.

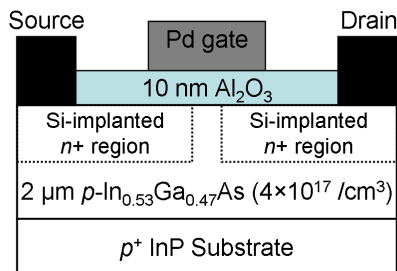


Fig. 1. Schematic cross-sectional diagram of a surface-channel In<sub>0.53</sub>Ga<sub>0.47</sub>As MOSFET with a 10-nm thick ALD Al<sub>2</sub>O<sub>3</sub> gate dielectric.

A 10-nm-thick  $\text{Al}_2\text{O}_3$  gate oxide film was formed by ALD using alternating pulses of  $\text{Al}(\text{CH}_3)_3$  (TMA) and  $\text{H}_2\text{O}$  precursors at  $250^\circ\text{C}$ . The source and drain (S/D) regions were selectively implanted with a Si dose of  $1 \times 10^{14}/\text{cm}^2$  at  $80\text{ keV}$  and  $1 \times 10^{14}/\text{cm}^2$  at  $30\text{ keV}$ . Implant activation was achieved by rapid thermal anneal (RTA) at  $600^\circ\text{C}$  for 15 s in a  $\text{N}_2$  atmosphere. A 140-nm-thick  $\text{SiO}_2$  field oxide was formed by electron beam evaporation and liftoff to minimize the gate pad capacitance. A 200-nm-thick Pd gate was defined by electron beam evaporation and liftoff. Non-self-aligned ohmic contacts were defined by lithography, selective wet etching of the  $\text{Al}_2\text{O}_3$  in dilute HF and electron beam evaporation of a Au (14 nm)/Ge (14 nm)/Au (14 nm)/Ni (11 nm)/Au (200 nm) metal stack [9]. Finally, a forming gas (5%  $\text{H}_2$ /95%  $\text{N}_2$ ) anneal treatment was carried out in an open tube furnace at  $300^\circ\text{C}$  for 30 min.

### III. RESULTS AND DISCUSSION

The  $\text{In}_{0.53}\text{Ga}_{0.47}\text{As}$  MOSFETs exhibit well behaved transfer and output characteristics, as shown in Fig. 2 (a) and (b), respectively. A threshold voltage,  $V_T$ , of  $0.43\text{ V}$ , a subthreshold swing,  $SS$ , of  $150\text{ mV/dec.}$ , an  $I_{ON}/I_{OFF}$  ratio of  $\sim 10^4$  and a source/drain resistance,  $R_{SD}$ , of  $103\text{ }\Omega$  were obtained.

Fig. 3 shows the  $C_{gc}$ ,  $C_{gb}$ ,  $C_g-V_g$  characteristics, obtained from split  $C-V$  measurements using an ac signal frequency of  $2\text{ MHz}$  and a temperature of  $-50^\circ\text{C}$ . The  $C_{gc}$ ,  $C_{gb}-V_g$  characteristics were corrected for the overlap and gate pad parasitic capacitances using the method reported in [10]. The  $C_g-V_g$  characteristics were obtained from the concatenation of  $C_{gc}-V_g$  and  $C_{gb}-V_g$ .

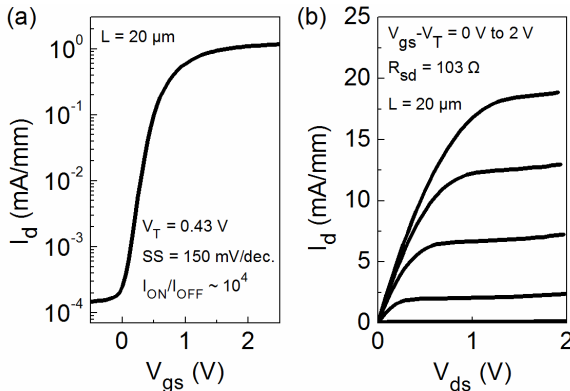


Fig. 2. (a) Log  $I_d-V_{gs}$  at  $V_{ds} = 50\text{ mV}$  and (b)  $I_d-V_{ds}$  for  $V_{gs}$  ranging from  $0\text{ V}$  to  $2\text{ V}$  obtained on a  $20\text{-}\mu\text{m}$ -gate length and  $50\text{-}\mu\text{m}$ -gate width device. The MOSFET features a  $V_T$  of  $0.43\text{ V}$ , a  $SS$  of  $150\text{ mV/dec.}$ , an  $I_{ON}/I_{OFF}$  of  $10^4$  and a  $R_{SD}$  of  $103\text{ }\Omega$ .

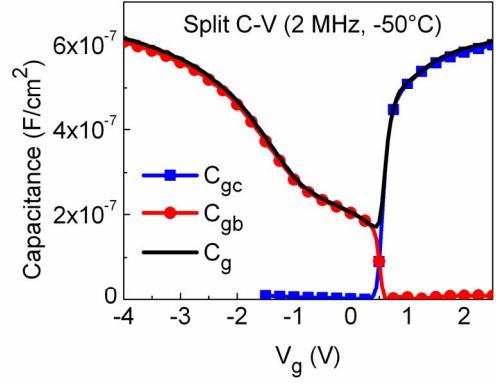


Fig. 3.  $C_{gc}$ ,  $C_{gb}$ ,  $C_g-V_g$  characteristics, obtained from split  $C-V$  measurements using an ac signal frequency of  $2\text{ MHz}$  and a temperature of  $-50^\circ\text{C}$ . The  $C_{gc}$ ,  $C_{gb}-V_g$  characteristics were corrected for the overlap and gate pad parasitic capacitances using the method reported in [9]. The  $C_g-V_g$  characteristic was obtained from the concatenation of  $C_{gc}-V_g$  and  $C_{gb}-V_g$ .

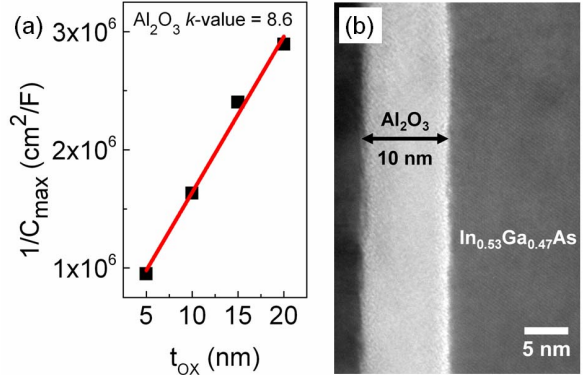


Fig. 4. (a) Inverse of maximum accumulation capacitance,  $1/C_{max}$ , versus oxide thickness,  $t_{ox}$ , for  $\text{Al}_2\text{O}_3/\text{In}_{0.53}\text{Ga}_{0.47}\text{As}$  MOSCAPs with  $t_{ox}$  ranging from  $5\text{ nm}$  to  $20\text{ nm}$ . (b) Cross sectional HRTEM image through the gate stack region of the MOSFET. A  $C_{ox}$  of  $7.6 \times 10^{-7}\text{ F/cm}^2$  was obtained based on the extracted  $\text{Al}_2\text{O}_3$   $k$ -value of  $8.6$  and the measured  $t_{ox}$  of  $10\text{ nm}$ .

The  $\text{Al}_2\text{O}_3$  dielectric constant,  $k$ , and the  $\text{Al}_2\text{O}_3$  film thickness,  $t_{ox}$ , were extracted in order to allow accurate QS  $C-V$  simulation. The  $\text{Al}_2\text{O}_3$   $k$ -value (8.6) was obtained from the slope of the capacitance equivalent thickness in accumulation versus the oxide thickness for  $\text{Al}_2\text{O}_3/\text{In}_{0.53}\text{Ga}_{0.47}\text{As}$  MOSCAPs with  $\text{Al}_2\text{O}_3$  thicknesses ranging from  $5\text{ nm}$  to  $20\text{ nm}$  (Fig. 4 (a)). The cross-sectional high resolution transmission electron microscopy (HRTEM) image through the gate oxide region confirmed a  $t_{ox}$  of  $10\text{ nm}$  (Fig. 4 (b)). The measured MOSFET gate oxide thickness combined with the extracted  $\text{Al}_2\text{O}_3$   $k$ -value yields a MOSFET oxide capacitance,  $C_{ox}$ , of  $7.6 \times 10^{-7}\text{ F/cm}^2$ .

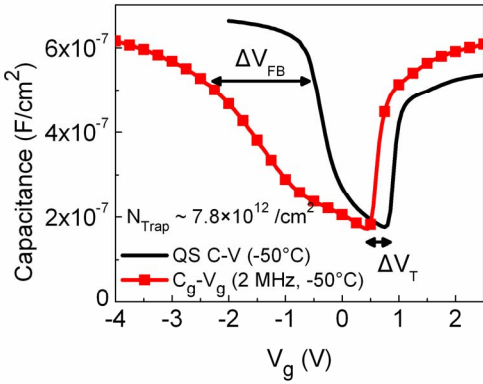


Fig. 5. Comparison of the  $C_g$ - $V_g$  characteristics, measured at 2 MHz and at  $-50^\circ\text{C}$ , to the theoretical QS  $C$ - $V$  characteristics at  $-50^\circ\text{C}$ , obtained from a self-consistent Poisson-Schrödinger simulation. An integrated  $N_{\text{Trap}}$  of  $7.8 \times 10^{12} / \text{cm}^2$  and an  $N^+$  of  $1.4 \times 10^{12} / \text{cm}^2$  were extracted from this comparison.  $\Delta V_{\text{FB}} = V_{\text{FB},\text{theo}} - V_{\text{FB},\text{meas}}$  and  $\Delta V_T = V_{T,\text{theo}} - V_{T,\text{meas}}$ .

Fig. 5 compares the reconstructed  $C_g$ - $V_g$  characteristics obtained from split  $C$ - $V$  measurements, using an ac signal frequency of 2 MHz and a temperature of  $-50^\circ\text{C}$ , with the simulated QS  $C$ - $V$  at  $-50^\circ\text{C}$ . In the simulation, the work function of Pd on  $\text{Al}_2\text{O}_3$ , the  $\text{Al}_2\text{O}_3$  film thickness and  $k$ -value, and the  $p$ -In<sub>0.53</sub>Ga<sub>0.47</sub>As doping concentration were set to 4.7 eV [11], 10 nm, 8.6 and  $4 \times 10^{17} / \text{cm}^3$ , respectively. The negative voltage shift of the  $C_g$ - $V_g$  characteristics relative to the theoretical QS  $C$ - $V$  characteristics is attributed to the presence of fixed positive charges in the  $\text{Al}_2\text{O}_3$  gate oxide film. The stretch of the  $C_g$ - $V_g$  characteristics in depletion is due to the presence of interface traps located near the middle of the In<sub>0.53</sub>Ga<sub>0.47</sub>As band-gap [12], [7]. The experimental  $C$ - $V$  stretch out towards the accumulation region could result from a high interface trap density towards the In<sub>0.53</sub>Ga<sub>0.47</sub>As valence band edge and/or border traps present in the  $\text{Al}_2\text{O}_3$  [13]. Measuring the stretch of the  $C_g$ - $V_g$  characteristics relative to the theoretical QS  $C$ - $V$  allows the determination of the overall integrated trap density, irrespective of the nature of the traps, as the additional gate voltage difference between the flat band voltage to the threshold voltage on the experimental  $C_g$ - $V_g$  response when compared to the Poisson-Schrödinger QS  $C$ - $V$  simulation, relates directly to the density of interface traps and border traps integrated across the band gap<sup>1</sup>, as expressed in (1):

$$N_{\text{Trap}} = C_{\text{OX}} \times (\Delta V_{\text{FB}} - \Delta V_T) / q \quad (1),$$

where  $\Delta V_{\text{FB}} = V_{\text{FB},\text{theo}} - V_{\text{FB},\text{meas}}$ ,  $\Delta V_T = V_{T,\text{theo}} - V_{T,\text{meas}}$  and  $q$  is the charge of an electron.

The equivalent density of fixed oxide charges at the  $\text{Al}_2\text{O}_3/\text{In}_{0.53}\text{Ga}_{0.47}\text{As}$  interface can be determined using (2):

$$N^+ = C_{\text{OX}} \times \Delta V_T / q \quad (2).$$

A theoretical flat band capacitance,  $C_{\text{FB},\text{theo}}$ , of  $5.2 \times 10^{-7} \text{ F/cm}^2$  and a theoretical flat band voltage,  $V_{\text{FB},\text{theo}}$ , of  $-0.48 \text{ V}$  were obtained from the simulation. A measured flat band voltage,  $V_{\text{FB},\text{meas}}$ , of  $-2.43 \text{ V}$  was obtained, assuming that  $C_{\text{FB},\text{theo}} = C_{\text{FB},\text{meas}}$ . The measured threshold voltage,  $V_{T,\text{meas}}$ , of  $0.55 \text{ V}$  obtained from the split  $C$ - $V$  measurements differs slightly from that obtained from the  $I$ - $V$  measurements due to the measurement conditions and  $C$ - $V$  hysteresis exhibited by the  $\text{Al}_2\text{O}_3/\text{In}_{0.53}\text{Ga}_{0.47}\text{As}$  MOS structure. Indeed, all the  $C$ - $V$  measurements were obtained using a sweep from inversion to accumulation at  $-50^\circ\text{C}$ , while the  $I$ - $V$  measurements were performed the opposite way and at room temperature. Considering a theoretical threshold voltage,  $V_{T,\text{theo}}$ , of  $0.85 \text{ V}$  and a  $C_{\text{OX}}$  of  $7.6 \times 10^{-7} \text{ F/cm}^2$ , we calculated a  $N_{\text{Trap}}$  of  $\sim 7.8 \times 10^{12} / \text{cm}^2$  and an  $N^+$  of  $1.4 \times 10^{12} / \text{cm}^2$  using (1) and (2), respectively. The integrated  $N_{\text{Trap}}$  value of  $\sim 7.8 \times 10^{12} / \text{cm}^2$  obtained with this method is consistent with a density of interface traps,  $D_{IT}$ , of  $\sim 5.8 \times 10^{12} / \text{cm}^2 \cdot \text{eV}$  obtained from an analysis of the SS (of 150 mV/dec) of the surface-channel In<sub>0.53</sub>Ga<sub>0.47</sub>As MOSFET.

The Maserjian Y-function, [14], is of particular interest to the analysis of high- $k$ /In<sub>0.53</sub>Ga<sub>0.47</sub>As MOS systems. The expression of the Maserjian Y-function is shown in (3):

$$Y = (dC / dV_g) / C^3 \quad (3),$$

where  $C$  is the overall gate capacitance and  $V_g$  is the gate voltage. This method allows accurate extraction of  $V_T$ ,  $N_a$  and  $V_{\text{FB}}$ . Indeed, the Maserjian Y-function peaks at  $V_T$ , while its minimum,  $Y_{\min}$ , is used to obtain  $N_a$  and  $V_{\text{FB}}$  using (4) and (5), respectively:

$$Y_{\min} = -(q \times \epsilon_{\text{InGaAs}} \times N_a)^{-1} \quad (4),$$

$$Y(V_{\text{FB}}) = Y_{\min} / 3 \quad (5),$$

where  $\epsilon_{\text{InGaAs}}$  is the In<sub>0.53</sub>Ga<sub>0.47</sub>As dielectric constant. Fig. 6 compares the Maserjian Y-functions obtained from the experimental  $C_g$ - $V_g$  and the theoretical “defect free” QS  $C$ - $V$  characteristics. The  $V_T$  shift due to the positive oxide charge in the  $\text{Al}_2\text{O}_3$  is evident (Fig. 6).  $Y_{\min}$  and (4) yielded a  $N_a$  value of  $3.3 \times 10^{17} / \text{cm}^3$  (inset Fig. 6), in close agreement with the  $4 \times 10^{17} / \text{cm}^3$  specification given to the wafer supplier. The distortion observed on the experimental Maserjian Y-function in the 0 V to  $-0.5 \text{ V}$  voltage region is consistent with a  $D_{IT}$  peak located near the middle of the band gap, while the influence of a larger  $D_{IT}$  peak near the valence band or a distribution of oxide border traps is visible in the  $-0.5 \text{ V}$  to  $-2 \text{ V}$  voltage region. This distortion in the experimental Maserjian Y-function prevents the extraction of  $V_{\text{FB}}$ . Further investigations of the mechanisms responsible for the distortion are on-going.

<sup>1</sup> For a doping concentration of  $4 \times 10^{17} / \text{cm}^3$  in  $p$ -In<sub>0.53</sub>Ga<sub>0.47</sub>As, the flat band and threshold voltage conditions related to Fermi level positions are 0.04 eV away from the valence and conduction band edges, respectively. Therefore, selecting the flat band and threshold voltage conditions for  $4 \times 10^{17} / \text{cm}^3$   $p$ -In<sub>0.53</sub>Ga<sub>0.47</sub>As does span the majority of the band gap.

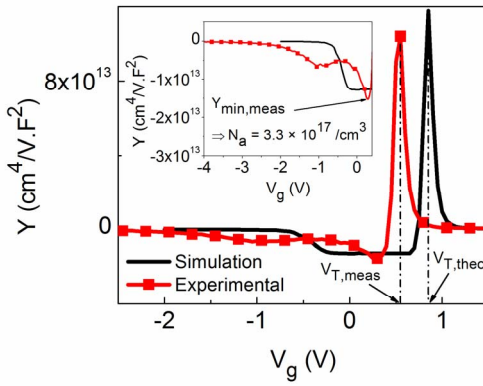


Fig. 6. Maserjian Y-function applied to the experimental  $C_g$ - $V_g$  characteristics and the simulated “defect free” QS  $C$ - $V$  characteristics. Inset: Extraction of a doping concentration,  $N_a$ , of  $3.3 \times 10^{17} / \text{cm}^3$  based on the minimum,  $Y_{\min,\text{meas}}$ , of the experimental Y-function.

The full paper will include the influence of interface traps on the theoretical Poisson-Schrödinger QS  $C$ - $V$  simulation and resulting Maserjian Y-function.

#### IV. CONCLUSION

We investigated interface and oxide defects in surface-channel  $\text{In}_{0.53}\text{Ga}_{0.47}\text{As}$   $n$ -MOSFETs using low-temperature high-frequency split C-V measurements and self-consistent Poisson-Schrödinger simulations. An integrated density of traps of  $\sim 7.8 \times 10^{12} / \text{cm}^2$  was obtained. This integrated density of traps, including  $\text{Al}_2\text{O}_3/\text{In}_{0.53}\text{Ga}_{0.47}\text{As}$  interface traps and the possible contribution of  $\text{Al}_2\text{O}_3$  border traps, is consistent with the MOSFET SS of 150 mV/dec. An equivalent surface density of fixed positive charges of  $1.4 \times 10^{12} / \text{cm}^2$  was also extracted. Further investigations of the mechanisms responsible for the distortion in both the reconstructed  $C_g$ - $V_g$  accumulation characteristics and the Maserjian Y-function are on-going.

#### ACKNOWLEDGMENT

This work was supported by Science Foundation Ireland under the FORME Strategic Research Cluster Award number 07/SRC/I1172F.

#### REFERENCES

- [1] M. Yokoyama, R. Iida, K. Sanghyeon, N. Taoka, Y. Urabe, H. Takagi, T. Yasuda, H. Yamada, N. Fukuhara, M. Hata, M. Sugiyama, Y. Nakano, M. Takenaka, and S. Takagi, "Sub-10-nm Extremely Thin Body InGaAs-on-Insulator MOSFETs on Si Wafers With Ultrathin  $\text{Al}_2\text{O}_3$  Buried Oxide Layers," *IEEE Electron Device Lett.*, vol. 32, no. 9, pp. 1218-1220, Sept. 2011.
- [2] C. Hock-Chun, L. Xinke, G. Xiao, and Y. Yee-Chia, "Silane and Ammonia Surface Passivation Technology for High-Mobility  $\text{In}_{0.53}\text{Ga}_{0.47}\text{As}$  MOSFETs," *IEEE Trans. Electron Devices*, vol. 57, no. 5, pp. 973-979, May 2010.
- [3] U. Singisetti, M. A. Wistey, G. J. Burek, A. K. Baraskar, B. J. Thibeault, A. C. Gossard, M. J. W. Rodwell, S. Byungha, E. J. Kim, P. C. McIntyre, Y. Bo, Y. Yu, D. Wang, T. Yuan, P. Asbeck, and L. Yong-Ju, " $\text{In}_{0.53}\text{Ga}_{0.47}\text{As}$  Channel MOSFETs With Self-Aligned InAs Source/Drain Formed by MEE Regrowth," *IEEE Electron Device Lett.*, vol. 30, no. 11, pp. 1128-1130, Nov. 2009.
- [4] N. Goel, D. Heh, S. Koveshnikov, I. Ok, S. Oktyabrsky, V. Tokranov, R. Kambhampatic, M. Yakimov, Y. Sun, P. Pianetta, C. K. Gaspe, M. B. Santos, J. Lee, S. Datta, P. Majhi, and W. Tsai, "Addressing the gate stack challenge for high mobility  $\text{In}_{x}\text{Ga}_{1-x}\text{As}$  channels for NFETs," in *IEDM Tech. Dig.*, 2008, pp. 1-4.
- [5] M. Caymax, G. Brammertz, A. Delabie, S. Sioncke, D. Lin, M. Scarrozza, G. Pourtois, W.-E. Wang, M. Meuris, and M. Heyns, "Interfaces of high-k dielectrics on GaAs: Their common features and the relationship with Fermi level pinning (Invited Paper)," *Microelectron. Eng.*, vol. 86, no. 7-9, pp. 1529-1535, Mar. 2009.
- [6] R. D. Long, B. Shin, S. Monaghan, K. Cherkaoui, J. Cagnon, S. Stemmer, P. C. McIntyre, and P. K. Hurley, "Charged Defect Quantification in  $\text{Pt}/\text{Al}_2\text{O}_3/\text{In}_{0.53}\text{Ga}_{0.47}\text{As}/\text{InP}$  MOS Capacitors," *J. Electrochem. Soc.*, vol. 158, no. 5, pp. G103-G107, Mar. 2011.
- [7] É. O'Connor, B. Brennan, V. Djara, K. Cherkaoui, S. Monaghan, S. B. Newcomb, R. Contreras, M. Milojevic, G. Hughes, M. E. Pemble, R. M. Wallace, and P. K. Hurley, "A systematic study of  $(\text{NH}_4)_2\text{S}$  passivation (22%, 10%, 5%, or 1%) on the interface properties of the  $\text{Al}_2\text{O}_3/\text{In}_{0.53}\text{Ga}_{0.47}\text{As}/\text{InP}$  system for *n*-type and *p*-type  $\text{In}_{0.53}\text{Ga}_{0.47}\text{As}$  epitaxial layers," *J. Appl. Phys.*, vol. 109, no. 2, p. 024101, Jan. 2011.
- [8] B. Brennan, M. Milojevic, C. L. Hinkle, F. S. Aguirre-Tostado, G. Hughes, and R. M. Wallace, "Optimisation of the ammonium sulphide  $(\text{NH}_4)_2\text{S}$  passivation process on  $\text{In}_{0.53}\text{Ga}_{0.47}\text{As}$ ," *Appl. Surf. Sci.*, vol. 257, no. 9, pp. 4082-4090, Feb. 2011.
- [9] P. A. F. Herbert, L. P. Floyd, J. I. Braddell, E. M. Baldwin, and W. M. Kelly, "The application of ohmic contacts to nanometric structures," *Microelectron. Eng.*, vol. 17, no. 1-4, pp. 541-546, Mar. 1992.
- [10] K. Romanjek, F. Andrieux, T. Ernst, and G. Ghibaudo, "Improved Split C-V Method for Effective Mobility Extraction in sub-0.1- $\mu\text{m}$  Si MOSFETs," *IEEE Electron Device Lett.*, vol. 25, no. 8, pp. 583 - 585, Aug. 2004.
- [11] A. Diligenti, and M. Stagi, "Tunnelling in aluminium/aluminium-oxide/palladium junctions: hydrogen-induced variations," *Electron. Lett.*, vol. 19, no. 18, pp. 717-718, Sept. 1983.
- [12] A. Ali, H. Madan, S. Koveshnikov, S. Oktyabrsky, R. Kambhampati, T. Heeg, D. Schlom, and S. Datta, "Small-Signal Response of Inversion Layers in High-Mobility  $\text{In}_{0.53}\text{Ga}_{0.47}\text{As}$  MOSFETs Made With Thin High-K Dielectrics," *IEEE Trans. Electron Devices*, vol. 57, no. 4, pp. 742-748, Apr. 2010.
- [13] G. Brammertz, H. C. Lin, K. Martens, A.-R. Alian, C. Merckling, J. Penaud, D. Kohen, W.-E. Wang, S. Sioncke, A. Delabie, M. Meuris, M. R. Caymax, and M. Heyns, "Electrical Properties of III-V/Oxide Interfaces," *ECS Transactions*, vol. 19, no. 5, pp. 375-386, May 2009.
- [14] G. Ghibaudo, S. Bruyere, T. Devouvre, B. DeSalvo, and E. Vincent, "Improved method for the oxide thickness extraction in MOS structures with ultrathin gate dielectrics," *Semiconductor Manufacturing, IEEE Transactions on*, vol. 13, no. 2, pp. 152-158, May 2000.